# A multiscale mechanobiological model of in-stent restenosis; deciphering the role of matrix metalloproteinase and extracellular matrix changes

Houman Zahedmanesh (PhD)[1], Hans Van Oosterwyck (PhD)[1], Caitríona Lally (PhD)[2]

*1. Department of Mechanical Engineering, Biomechanics Section, KU Leuven, Leuven, Belgium*

*2. Department of Mechanical and Manufacturing Engineering, Dublin City University, Dublin, Ireland*

Submitted to: Computer Methods in Biomechanics and Biomedical Engineering (CMBBE)

Corresponding author:

Dr. Houman Zahedmanesh

Department of Mechanical Engineering, Biomechanics Section (BMe)

KU Leuven,

Leuven, Belgium

Houman.Zahedmanesh@mech.kuleuven.be

Phone: +32 16 328990/328994

Fax: +32 16 3 27994

# A multiscale mechanobiological model of in-stent restenosis; deciphering the role of matrix metalloproteinase and extracellular matrix changes


## Abstract

Since their first introduction, stents have revolutionised the treatment of atherosclerosis, however the development of in-stent restenosis still remains the Achilles' heel of stent deployment procedures. Computational modelling can be used as a means to model the biological response of arteries to different stent designs using mechanobiological models whereby the mechanical environment may be used to dictate the growth and remodelling of vascular cells. Changes occurring within the arterial wall due to stent induced mechanical injury, specifically changes within the extracellular matrix have been postulated to be a major cause of activation of vascular smooth muscle cells and the subsequent development of in-stent restenosis. In this study a mechanistic multiscale mechanobiological model of in-stent restenosis using finite element models and agent based modelling is presented which allows quantitative evaluation of the collagen matrix turnover following stent induced arterial injury and the subsequent development of in-stent restenosis. The model is specifically used to study the influence of stent deployment diameter and stent strut thickness on the level of in-stent restenosis. The model demonstrates that there exists a direct correlation between the stent deployment diameter and the level of in-stent restenosis. In addition, investigating the influence of stent strut thickness using the mechanobiological model reveals that thicker strut stents induce a higher level of in-stent restenosis due to a higher extent of arterial injury. The presented mechanobiological modelling framework provides a robust platform for testing hypotheses on the mechanisms underlying the development of in-stent restenosis and lends itself for use as a tool for optimization of the mechanical parameters involved in stent design.



Keywords: In-stent restenosis, Multi-scale Mechanobiological Modelling, Agent Based Model (ABM), Finite Element Method (FEM), Matrix metalloproteinase (MMP), Extracellular matrix (ECM)

## 1. Introduction

Since their first introduction in 1985 by Palmaz et al. (1985), balloon-mounted vascular stents have revolutionised the treatment of atherosclerosis, and in particular coronary artery disease. Now over 25 years on, stents have undeniably become the gold standard in the non-invasive treatment of atherosclerosis with 3 million implanted worldwide each year (van Beusekom and Serruys 2010). While recent stent designs have offered significant improvements over their predecessors, one significant limitation in the long-term success of stents still remains, namely in-stent restenosis.

Following stent deployment, an over-zealous healing response broadly known as in-stent restenosis, may initiate within the arterial wall which can ultimately lead to renarrowing of the vessel due to excessive migration and proliferation of medial vascular smooth muscle cells (VSMC) towards the vessel lumen (Hoffmann and Mintz 2000; Lowe et al. 2002). During the expansion of the stent, high stresses induced by the stent cause injury to the artery which leads to thrombosis formation in the arterial wall and a cascade of inflammatory events. Close correlation has been found between the degree of arterial injury, the resulting inflammatory reaction and the neointimal thickness (Kornowski et al. 1998; Wieneke et al. 1999; Welt et al. 2002; Mitra et al. 2006). Therefore many studies have used the degree of injury caused by the implantation of a stent as an independent determinant for estimating the thickness of restenotic growth (Schwartz et al. 1992; Schwartz and Holmes 1994; Gunn et al. 2002). Given that the degree of vessel injury is a determining factor for in-stent restenosis it is consequently a key design consideration for stents. In this context, numerical modelling techniques are an efficient and powerful means to optimise stent design parameters in order to minimise stent induced arterial stresses and injury.

Several computational models of stent deployment have been developed in recent years which have elucidated further the mechanics of stent-artery interaction with the ultimate goal of reducing stent induced arterial stresses (Migliavacca et al. 2002; Lally et al. 2005; Holzapfel et al. 2005a; Wang et al. 2006; De Beule et al. 2008; Mortier et al. 2010; Zahedmanesh et al. 2010). The influence of several mechanical parameters such as stent strut thickness (Timmins et al. 2007; Zahedmanesh and Lally 2009), plaque composition (Pericevic et al. 2009) and bending in stented peripheral arteries (Early et al. 2008) have been studied. Balloon expandable stents have also been compared with self-expanding stents in terms of the level of stresses they induce within the arterial wall and hence the risk of arterial injury using finite element (FE) models (Migliavacca et al. 2004).

Moreover, computational modelling also provides a means to model the biological response to an implant using mechanobiological models whereby the mechanical environment may be used to dictate the growth and remodelling of vascular cells (Boyle et al. 2011; Zahedmanesh and Lally 2012). In-stent restenosis is intrinsically a multi-scale phenomenon which necessitates a multi-scale modelling approach. Therefore, multi-scale approaches utilising discrete methods such as cellular automata (CA) (Masselot and Chopard 1998; Ilachinski 2001) and agent based models (ABM) (Wooldridge 2002; Walker et al. 2004) have recently received particular attention for modelling in-stent restenosis *by developing multiscale ABM based platforms (Evans et al. 2008; Caiazzo et al. 2009; Tahir et al. 2011). The approach adopted in these studies* is mainly based on discrete methods, whereas, a hybrid approach can also be adopted by combining continuum methods such as FEM and discrete methods. FEM is particularly advantageous given that it has proved to be a robust method for quantification of arterial stresses and has been successfully utilised

for patient specific modelling of stent-artery interaction (Zahedmanesh et al. 2010; Gijsen et al. 2008). As an example, Boyle et al. (2011) used FE simulations of stent deployment to quantify damage within a stented artery and subsequently used a lattice based CA approach to simulate the biological response of the artery to this stent induced damage quantified by the FE model (Boyle et al. 2010; Boyle et al. 2011).

After stent deployment, vessel injury by the stent struts leads to the activation of medial VSMC, which are in a quiescent and contractile phenotype in the uninjured artery, to a synthetic phenotype. This change of phenotype is followed by migration and proliferation of dedifferentiated medial VSMC towards the lumen and lesion formation, see Figure 1, (Wieneke et al. 1999; Babapulle and Eisenberg 2002; Welt et al. 2002; Mitra et al. 2006). A myriad of factors are involved in the modulation of VSMC phenotype from a quiescent to synthetic phenotype, including endothelial damage and denudation during stent deployment which is followed by adhesion of thrombocytes which express mitogenic chemokines and result in the chemotactic migration and proliferation of VSMC towards the lumen. Nevertheless, mitogens are not the only factor involved in the phenotypic modulation and activation of medial VSMCs. For example, exogenously added fibroblast growth factor (FGF) increases VSMC proliferation in injured arteries, whereas it does not influence VSMC proliferation in uninjured arteries (Lindner and Reidy 1991; Reidy and Lindner 1991). This observation suggests that other changes related to injury within the vessel may also be involved in the regulation of VSMC activation. In this context, the extracellular matrix (ECM) changes following vessel injury seems to be a key regulator of VSMC phenotype and activation. Thyberg et al. (1997) showed that the medial VSMCs in injured rat carotid arteries with a synthetic phenotype were enclosed by an incomplete basement membrane compared to normal arteries. These cells were found to migrate into the

intima via holes in the internal elastic lamina and to form the neointimal tissue. Ultimately the VSMC resumed a contractile phenotype as the neointima reached its final size with development of a complete basement membrane. Based on these observations Thyberg et al. (1997) suggested that basement membrane components promote differentiation of VSMC towards a quiescent and contractile phenotype whereas their degradation leads into VSMC dedifferentiation and activation. Collagen type IV constitutes about 50% of the VSMC's basement membrane and is crucial for basement membrane stability and assembly (Hirose et al. 1999; Aguilera et al. 2003; Monaco et al. 2006). In addition, collagen type I and type III are abundant in the medial layer of arteries which are oriented in the circumferential direction and maintain the mechanical integrity and stability of arteries under high loads (von der Mark 1981). Migration and proliferation of VSMCs in cultured human saphenous vein has been directly related to degradation of basement membrane type IV collagen showing that all VSMCs which migrated to the neointima lacked collagen type IV (Aguilera et al. 2003; Adiguzel et al. 2009). In addition to basement membrane collagen type IV, it has been shown that fibrilar collagen type I promotes a quiescent and contractile VSMC phenotype whereas its degradation promotes a synthetic VSMC phenotype (Adiguzel et al. 2009). Clearly therefore, in addition to the basement membrane collagen type IV which is a network-like matrix, fibrilar collagens such as collagen type I which maintain the mechanical integrity of arteries are also implicated in regulation of VSMC response in the arterial wall. Given that fibrilar collagen type I and III, bear the most significant share of the mechanical load at high extensions, damage due to stent deployment is likely to be most significant in the collagen matrix, specifically fibrilar collagen type I & III.

Matrix degrading metalloproteinase (MMPs) have been found to regulate migration, proliferation and survival of VSMCs within the vessel wall (Newby 2006). Basement membrane degrading MMPs, i.e gelatinases MMP-2 (Gelatinase A) and MMP-9 (Gelatinate B), both degrade collagen type IV (Newby 2006) and MMP2 also degrades fibrilar collagen type I and III (Doronzo et al. 2005; Newby 2006). A study by (Asanuma et al. 2003) showed that stationary mechanical stretch, increases gelatinase expression in cultured human VSMCs suggesting that local increases in stationary mechanical strain resulting from stenting, hypertension, or atherosclerosis may lead to enhanced matrix degradation by VSMCs. Mechanical injury upregulates MMP-2 production which is a major proteinase of the basement membrane (James et al. 1993; Bendeck et al. 1994; Southgate et al. 1996; George et al. 1997) and so does mechanical stretch (Asanoma et al. 2002; Grote et al. 2003). In addition, injury has been shown to upregulate MMP-2 and MMP-9 expression and activity in surgically prepared human saphenous veins with damage to the endothelium and medial layer (George et al. 1997). In a separate study, a significant increase in MMP-2 activity was observed between 4 and 14 days following balloon catheter arterial injury in rat (Bendeck et al. 1994).

The aforementioned observations clearly signify the important role of collagen as the main constituent of ECM and basement membrane in arteries and motivate utilising computational models for quantitative evaluation of ECM dynamics. In this study, a hybrid mechanobiological model is utilised to decipher the role of changes occurring within the collagen matrix following stent deployment and its implications for in-stent restenosis. Given that MMP-2 cleaves a wider range of collagen types compared to MMP-9, including degradation of fibrilar collagen type I and III in addition to collagen type IV, in this study MMP expression by VSMCs and its effect on the collagen matrix was calibrated against experimental data on MMP-2. As such, the

term ECM in this article refers interchangeably to the collagen matrix and the term MMP specifically refers to MMP-2.

## 2. Methods and Materials

### *2.1 Model Overview*

A mechanobiological modelling framework was developed which comprises of two main coupled modules, (i) a module based on FEM that quantifies von Mises stresses to estimate the level of arterial damage due to stent deployment and (ii) a biological modelling module based on a lattice free ABM that simulates the key responses of VSMC growth, i.e. migration, proliferation and ECM degradation and synthesis in the arterial wall in response to the stent induced damage quantified using the FE analysis, see Figure 2. This modelling framework has been previously successfully applied to study remodelling in tissue engineered blood vessels where the framework was outlined in detail (Zahedmanesh and Lally 2012).

The simulation starts in the FE module where the value of the initial stent induced damage is quantified and is transferred to the ABM where the response of VSMCs and ECs is simulated. A custom-written routine was developed using python programming language to enable communication between the FE software Abaqus (Simulia, Providence, RI, USA) and the agent-based modelling framework BREVE (www.Spiderland.org). The ABM was programmed using the STEVE language specific to the BREVE agent-based modelling framework.

#### *2.1.1 Finite Element Model*

An axisymmetric hyperelastic FE model of an artery was developed which is composed of 3,040 equilateral rectangular axisymmetric elements (Abaqus type CAX4RH). *The*

*outer diameter of the mid-LAD (middle segments) coronary arteries is reported to be 4.5±0.3 (SD) mm with a total wall thickness of 0.87±0.23 (SD) mm (Holzapfel et al. 2005). In this study the arterial geometry was modelled as 8mm long with a thickness of 0.67 mm and a luminal diameter of 2.46 mm and was discretised by 190 elements longitudinally and 16 elements radially which was chosen based on mesh sensitivity studies. A pressure of 100 mmHg was applied to the luminal surface of the artery to take the mean arterial blood pressure into account whilst the two ends of the artery were longitudinally tethered. Application of the mean physiological blood pressure increased the luminal vessel diameter to 3.92 mm.* The influence of stent struts was modelled by application of a rigid body displacement into the artery representing a stent strut, see Figure 3. Coronary stents have been manufactured with strut thicknesses ranging from 0.04 mm to 0.2 mm (Garasic et al. 2000; Kastrati et al. 2001; Tarashima et al. 2009). In order to study the influence of stent strut thickness two types of struts with rectangular cross section where deployed, a thin strut with a width of 0.085 mm and a thick strut with a width of 0.17 mm. *The thin strut stent was deployed to obtain three different final luminal diameters of 4.3 mm, 4.7 mm and 5.1 mm to study the influence of strut penetration into the arterial wall. This leads to luminal diameter expansion ratios of 1.1, 1.2 and 1.3 respectively compared to the vessel diameter under mean physiological blood pressure of 100 mmHg.*

*The following Ogden hyperelastic equation, based on the stress-strain response of medial and adventitial layers of human coronary arteries reported by Holzapfel et al. (2005), was used to model the stress-strain response of the artery with a media to adventitia thickness ratio of 1.67 and assuming incompressibility of the arterial wall (Ogden 1972).*

$$\overline{U} = \sum_{i=1}^{3} \frac{2\mu_i}{\alpha_i^2}(\lambda_1^{-\alpha_i} + \lambda_2^{-\alpha_i} + \lambda_3^{-\alpha_i} - 3)$$

where, $\overline{U}$ is the deviatoric strain energy density, $\lambda_i$ denotes the deviatoric principle stretches and $\mu_i$ and $\alpha_i$ are the hyperelastic constants, see table 1.

*2.1.2 Damage/injury quantification*

Damage/injury level within the stented artery was quantified with a continuous linear range of 0 to 1. It was assumed that damage was mainly induced within the collagenous constituent of the ECM given its abundance within the arterial wall and the fact that collagen fibres have the highest load bearing capacity within the arterial wall. Currently there is a lack of quantitative data on the stress/strain levels known to cause arterial injury and initiation of pathological responses such as intimal hyperplasia. However some experimental data on the stress-strain response of human coronary arteries and its ultimate tensile stress is available and when used in combination with FE modelling it can be used to provide some quantitative estimation of arterial damage/injury. In this study we used a sigmoid function to describe damage/injury in the arterial wall as a function of von Mises stresses. This is a simplifying assumption which represents a very first approach to modelling damage within the artery. At an arterial pressure range of 0-120 mmHg there should be no damage/injury within the arterial wall given that 120 mmHg is the physiological systolic pressure. An FE model of the artery loaded with a luminal pressure of 120 mmHg was solved and the von Mises stresses within the arterial wall where found to have a maximum value of 140 kPa, up to which no arterial injury would be induced within the arterial wall. In addition, a value of 1 was assigned for the damage in the elements where von Mises stresses exceeded 252kPa. This value was chosen given that the medial layer in human coronary arteries has been reported to have

an ultimate tensile strength of 446±194 kPa in the circumferential direction (Holzapfel et al. 2005b). Therefore, 252 kPa represents the lowest value of ultimate tensile strength of these tissues before failure, i.e. one standard deviation below the mean for medial tissue, and it is therefore deemed a conservative choice of stress level for maximal injury associated with a damage value of 1. It should also be noted that the constitutive model applied for modelling this arterial response to blood pressure was also obtained based on the stress-strain response of human coronary arteries presented in Holzapfel et al. (2005b). A sigmoid function was fit to the data to define the level of arterial injury as a continuous function of von Mises stresses, as follows, (also see Figure 4):

$$Damage = \frac{0.1103}{0.1087 + e^{-0.1087(S_{Mises}(kPa)-200)}}$$

This model represents a simplified first approach to modelling damage/injury within the artery based on their stress-strain response. More sophisticated models of arterial injury based on the biological response of arteries to damage, i.e. thrombosis formation and ECM damage are needed, however obtaining such quantitative data on human coronary arteries still remains a daunting challenge. Nevertheless, the ABM-FE model presented here can incorporate any range of damage models, with damage calibrated against clinical or experimental data, such as that proposed by Boyle et al. (2011).

*2.1.3 Agent based model*

An agent based model of the artery was developed with VSMCs randomly distributed throughout the artery's geometrical domain and the ECs lining the luminal surface. The initial density of VSMCs was set to 950 cells/mm$^2$ consistent with the data reported for aged atheronecrotic human coronary arteries by (Tracy 1997). 223 ECs were evenly

distributed to line the lumen of the artery confluently given the dimension of ECs which were modelled as spheres with a radius of 0.01787 mm, see table 2.

Following the FE analysis, the values of the arterial damage were calculated based on the value of von Mises stresses quantified at the centroid of each element of the FE model and were exported to the ABM module similar to the approach previously outlined in Zahedmanesh and Lally (2012) assuming that the injury occurs once and in the initial stent expansion procedure.

In the agent-based model, an m×n matrix A is defined for the element damage values where m = the number of FE elements in the longitudinal direction and n = the number of FE elements in the radial direction. Each component of the matrix takes the value of damage calculated based on the quantified value of von Mises stress at the centroid of the corresponding FE element. Hence, at each point in the ABM domain, the value of the corresponding damage can be queried by referring to the related matrix component based on the coordinates of the point. The time step for the ABM simulations was set to 1 h given that the experimental data used on cell processes such as cell migration, proliferation, matrix and MMP synthesis were available in a per hour basis.

The damage induced in the vessel wall due to high stresses upregulates MMP synthesis by VSMCs which consequently causes degradation of the ECM. Initially VSMC were assumed to be in a quiescent and contractile phenotype. Degradation of ECM modulates their differentiation toward a synthetic phenotype at the site of damage which ultimately triggers their migration and proliferation, i.e. cells are only allowed to migrate and proliferate when their ECM is degraded to lower than the normal value of ECM in the healthy arteries which for collagen is a value of approximately $3.1\times10^{-4}$ μg/cell (Hahn et al. 2007). This is also the initial value of collagen in the model and

corresponds to a value of $6.2\times10^{-4}$ μg/element given that initially two VSMCs reside in each element.

ECM cleavage and degradation due to MMP upregulation reduces the value of the initially induced damage given the assumption that damage is induced within the ECM, and hence it functions as a negative feedback mechanism reducing the neointimal growth rate. In practice this was implemented by choosing the rate of damage removal by MMPs based on the fraction of ECM degraded by MMPs, see Table 2. This is a plausible assumption which has been previously utilised by Boyle et al. (2011) due to the fact that the collagen matrix within the arteries bears the most significant share of load at high arterial extensions and hence damage due to supra-physiological loads will be most significant within the collagen matrix.

Where the value of ECM was reduced to lower than the normal ECM value per cell in arteries due to damage and MMP activity, VSMCs were activated and switched to a synthetic phenotype i.e. they started to migrate, proliferate and synthesise ECM. The direction of migration and proliferation of VSMCs was chosen to be random, while contact inhibition between cells was enabled to prevent cell overlap in the model. A further development of this model could be to implement directed migration of cells towards higher chemokines, i.e. growth factors, however this was deemed beyond the scope of this model given that it requires calculation of the advective and diffusive transport of growth factors within the arterial wall which is a considerable challenge. VSMCs could proliferate as long as they retained synthetic phenotype i.e. the amount of ECM within the arterial wall was below $6.2\times10^{-4}$ μg/element which is the value of collagen in normal arteries. Once the damage stimulus recessed and synthetic VSMCs synthesised ECM and increased its value to this threshold, they switched back to the quiescent phenotype. In addition, a maximum VSMC density of 1432 cells/mm$^2$ was

allowed, consistent with the VSMC density in fibroplastic intimal thickness of human coronary arteries as reported in Tracy (1997), above which cell proliferation ceased. The influence of ECs was included based on the measurements reported in Matsusaki et al. (2011) where it is shown that the distance of NO diffusion from the endothelium to the underlying VSMC layers is approximately 60 μm. As such, if an endothelial cell was present within a neighbourhood of 60 μm radius from a VSMC, the VSMC switched back to the quiescent phenotype even if the value of ECM per VSMC was lower than the threshold ECM value, i.e. $6.2\times10^{-4}$ μg/element. The ECs were denuded in the beginning of the simulation where arterial damage occurred and ECs adjacent to the damaged area were allowed to proliferate back onto the damaged area until full re-endothelialisation. Endothelial cells were only allowed to migrate and proliferate on the luminal surface of the artery i.e. on top of VSMCs. The proliferating VSMCs synthesised ECM and gradually switched back to the contractile phenotype once their value of ECM reached the ECM threshold value which is the value of collagen in normal arteries, see Figure 1. The variables for ECM and MMPs were updated at each element based on the production reaction formula provided in table 2.

## 3. Results

The dynamics of events occurring within the arterial wall following expansion of the 0.085 mm thickness strut to a diameter of *4.7 mm* and the consequent response of VSMCs is shown in Figure 5 and 6. The changes in the damage field initially induced within the artery, the synthesis of MMPs and ECM changes are shown. One week following stent deployment, synthesis of MMP-2 reached a maximum of 0.015 pg/element which led to increased degradation of collagen. The maximum amount of collagen per VSMC dropped 33% from the initial state in the vicinity of the stent strut

after 2 weeks. At the same time, along with the degradation of the collagen matrix, VSMCs were also activated and their number started to increase 2 days following stent deployment. The increase in MMP synthesis reached its maximum 1 week post deployment when it subsequently started to revert to normal levels, decreasing 80% of the maximum level by the end of day 14. This can be explained based on the changes occurring within the damage field in the artery as shown in Figure 6. The increase in the MMP concentration and the consequent ECM degradation reduced the maximum of damage initially induced within the artery by more than 90%, by 12 days post deployment. As MMP synthesis is dependent on the arterial damage, the removal of damage following 2 weeks leads to a reduction in MMP concentration. Interestingly, this is consistent with the outcome of organ culture experiments conducted on damaged human saphenous vein (George et al., 1997).

Two cases were investigated using the developed mechanobiological model where the arterial response to deployment of a single stent strut was modelled in terms of development of in-stent restenosis in order to decipher the influence of stent deployment diameter and stent strut thickness. In the first case study the influence of deployment diameter was explored using the mechanobiological model where a stent strut was expanded to obtain three different luminal diameters of *4.3 mm*, representing a case with a mild strut penetration into the arterial wall, *4.7 mm*, representing a case with a medium strut penetration and *5.1 mm*, representing a case with a deep strut penetration into the arterial wall, see Figure 7. In a separate case, the influence of strut thickness was studied by comparing two strut geometries, strut thicknesses of 0.085 mm and 0.17 mm. The response of the artery to stent induced damage was compared in terms of development of in-stent restenosis in all of the different cases, see Figure 8, 9 and 10.

*Investigating the influence of stent deployment diameter clearly showed increased VSMC activation and luminal ingrowth with increasing diameter, see Figure 8. When the strut was deployed to a final diameter of 4.3 mm minimal VSMC activation and ingrowth occurred and endothelial repair was complete within three weeks. However, where the strut was deployed to obtain a final diameter of 4.7 mm significant VSMC activation and ingrowth was observed and the total VSMC number increased 19% after 28 days when compared to the uninjured state. The cell number curve was biphasic with an initial abrupt growth phase lasting approximately 21 days followed by a more stable growth phase. Complete re-endothelialisation occurred within 26 days when full lesion stabilisation occurred. A further increase in stent deployment diameter to a luminal diameter of 5.1 mm caused a significantly higher increase in VSMC ingrowth leading into a 40% increase in the VSMC number compared to the uninjured state. Interestingly, the model predicts that when the vessel is expanded to 5.1 mm, i.e. deep strut penetration into the arterial wall, not only is the final lesion size and cell ingrowth significantly larger compared to 4.3 and 4.7 mm deployment diameters, but the timescale of in-stent restenosis development is also lengthened with full re-endothelialisation and lesion stabilisation delayed until day 42, see Figure 8. In Figure 10, one can compare the influence of deployment diameter on changes occurring within the ECM. The results illustrate that the extent of matrix degradation in the vicinity of the stent struts increases when the stent strut is deployed to a higher diameter. In addition a higher amount of ECM is deposited within the lumen and the time to stabilisation of the lesion is delayed when the strut is deployed to a higher diameter, see Figure 10.*

*In order to elucidate the influence of stent geometry, i.e. strut thickness, two stent struts with different thicknesses were deployed to the same final vessel luminal*

*diameter of 4.7 mm in separate analyses. The results showed that VSMC numbers were 4% higher where the thicker strut was used and complete healing and stabilisation of in-stent restenosis was also delayed by 14 days when the thicker strut was deployed, see Figure 9.*

## 4. Discussion

As discussed earlier, collagen turnover following arterial injury plays a key role in regulating the activation of VSMCs. Interestingly the model results on collagen changes were found to be consistent with the outcome of organ culture studies on damaged human saphenous vein which showed that although in the first 2 days following injury there was a significant increase in degradation compared to uninjured veins, at days 12-14 there was no significant difference in degradation when compared to healthy tissue (George et al. 1997). The injury in the aforementioned study involved endothelial denudation and damage to the media which is consistent with the type of damage/injury that is induced in arteries due to stenting. This suggests that MMP concentration should regress following 12-14 days from the initial injury and clearly therefore damage, which is the stimulus for MMP synthesis, should be fully removed 2 weeks post injury. This is consistent with the time scales of MMP synthesis, collagen degradation and damage removal predicted by the presented mechanobiological model.

When the influence of the stent deployment diameter was studied by expanding the stent strut to increasing diameters, the model predicted that a direct relationship between the stent deployment diameter and the level of in-stent restenosis exists which is also consistent with the outcome of several *in-vivo* studies (Kornowski et al. 1998; Lowe et al. 2002; Gunn et al. 2002; Houbballah et al. 2011). As such, a subtle balance exists between the deployment diameter and the level of in-stent restenosis. If the stent

deployment diameter is increased to obtain a higher patency in the surgical procedure, the resulting level of in-stent restenosis will also increase which could ultimately compromise the efficiency of the procedure. In a recent study on development of in-stent restenosis, Timmins et al. (2011) showed that a direct correlation exists between wall stresses and the level in-stent restenosis. Higher expansion diameters lead to higher vessel stresses and clearly therefore a higher in-stent restenosis. As a result, it is crucial to determine a stent expansion ratio which would not trigger high in-stent restenosis and yet would reasonably improve the patency of the vessel. *Nevertheless, in practice the expansion ratio throughout the stent is inevitably inhomogeneous depending on the geometry of the plaque and the degree of stenosis with values which could exceed 1.3 at the site of stenosis and lower values near the end of the lesion.*

It should be noted that in the presented model endothelial denudation was assumed to only occur in the damaged area in the vicinity of a single strut, however, in the clinical cases full endothelial denudation usually occurs due to balloon artery interaction throughout the length of the stent and as such, re-endothelialisation and stabilisation of the lesion could take longer. Clearly therefore, the loss of patency due to in-stent restenosis might be even more significant depending on the extent of endothelial damage which renders determination of a safe stent expansion diameter for prevention of VSMC activation a critical choice. In addition, in recent years, several clinical trials have identified stent strut thickness as an independent predictor of restenosis (Kastrati et al., 2001; Briguori et al. 2002; Pache et al. 2003). A clear conclusion from the many clinical studies on stent strut thickness is that stents with thinner struts have a lower restenosis rate (Morton et al. 2004). Consistent with these experimental findings, the mechanobiological model also predicted a higher luminal ingrowth and number of VSMCs when a thicker strut stent was used, see Figure 7 & 9.

The observed differences in the level of in-stent restenosis predicted by the model when the stent strut was deployed to different diameters and also when a thicker strut stent was used, can be directly correlated to the mechanical stresses induced within the arterial wall and the corresponding levels of arterial injury, see Figure 7. *Where the stent was deployed to obtain a final luminal diameter of 4.3 mm, the maximum von Mises stresses within the arterial wall reached 367 kPa. Increasing the deployment diameter to 4.7 mm luminal diameter the maximum von Mises stresses increased to 868 kPa showing a 2.4 fold increase. When the diameter was increased even further to 5.1 mm the stresses increased to 1,609 kPa showing a 4.4 and 1.8 fold increase compared to 4.3 mm and 4.7 mm luminal diameters, respectively.* Obviously, this abrupt increase in the level of vessel stresses and the level of in-stent restenosis is due to the nonlinear stress-stiffening response of arteries. In this context, Zahedmanesh and Lally (2009) studied the influence of stent strut thickness on the vessel wall stresses by more sophisticated 3D FE simulations of stent deployment and showed that stents with thicker struts induce higher chronic stresses within the vessel wall and also pose a higher risk of injury in the vessel during expansion. The study showed that the stents fabricated with the same material but with thicker struts, recoil less compared to thinner strut stents and as a result in practice the thickness of the struts can also influence their final deployment diameter (Zahedmanesh and Lally 2009). Clearly therefore, the influence of strut thickness can be considered to be two-fold; on the one hand, as shown by the presented mechanobiological model, a thicker strut will induce more extensive damage to the arterial wall due to its thicker contact area with the artery and on the other hand, thicker struts recoil less compared to thinner struts and consequently the final deployment diameter obtained using thicker struts will be higher in practice. Nevertheless, hemodynamic factors may also be involved in the higher restenosis rates

using thicker stents. Specifically, thicker struts have been shown to lead to increased blood flow perturbations including significantly larger recirculation zones and altered shear stress patterns in the vicinity of struts which can potentially contribute to restenosis (Duraiswamy et al. 2007).

In order to further elucidate the influence of re-endothelialisation, a case where ECs could proliferate normally was compared with a case where ECs were not permitted to proliferate, see Figure 11. The results clearly show that re-endothelialisation is crucial for stabilisation of in-stent restenosis. Although for 21 days post stent deployment the number of VSMCs increased in the same manner for both models, with the growth curves overlapped, without re-endothelialisation in-stent restenosis never stabilised and the lesion grew until full occlusion of the artery, see Figure 11. The importance of ECs is most significant in terms of the behaviour of proliferating VSMCs in the vicinity of the lumen in the restenosis area given that in contrast to the deeper VSMCs, the ECM value for the VSMCs in the vicinity of the lumen in the restenosis area could not reach the threshold value without re-endothelialisation due to their persistent luminal ingrowth. Re-endothelialisation modulated the phenotype of VSMCs situated in the vicinity of the lumen boundary to quiescence and ensured stabilisation of the restenotic growth.

Due to the complexity and diversity of the factors involved in the development of in-stent restenosis, the study also has its limitations. Hemodynamic parameters such as shear stress have been postulated to be involved in the development of in-stent restenosis. Specifically ECs which line the lumen of arteries are widely known to be sensitive to blood flow perturbations and hence the changes occurring in the blood flow due to stent strut geometry, change of vessel diameter and stenosis may also influence cell behaviour (Wentzel et al. 2000 and 2001). Also, following injury other cell

populations such as thrombocytes are recruited in the damaged area which synthesise MMPs and along with ECs and VSMCs synthesise growth factors such as platelet derived growth factor (PDGF), transforming growth factor (TGF) and FGF, (Chabrier 1996). Nevertheless, as discussed earlier it has been shown that exogenously added fibroblast growth factor (FGF) increases VSMC proliferation in injured arteries, whereas it does not influence VSMC proliferation in uninjured arteries (Lindner and Reidy 1991; Reidy and Lindner 1991). Such an observation suggests that it is more likely that growth factors are not the key modulator of VSMC activation following injury but rather an amplifier of their active state characteristics. In terms of the damage/injury quantification, in this study a simple approach based on the stress-strain response of human coronary arteries and their ultimate tensile strength was used, however more sophisticated models need to be developed based on experimental studies whereby biological and microstructural changes in human arteries should be quantitatively related to increasing levels of mechanical stress/strain. Although its application to obtain human specific data constitutes a daunting challenge, in-vivo animal studies and also organ culture studies can be potentially conducted to provide better quantitative understanding of damage induced stenosis. *Even though in this study damage was assumed to be mainly induced in the collagen matrix as the main load bearing constituent of ECM, arterial cells could also be potentially damaged following stenting. Repopulation of the damaged areas with new cells is not however sufficient to stop lesion growth until a mature ECM is restored around VSMCs (Thyberg et al. 1997; Aguilera et al. 2003; Adiguzel et al. 2009). Therefore, dynamics of restenosis and lesion growth is more likely to be dominated by the dynamics of ECM turnover.*

Last but not least, the reduction of arterial compliance due to stenting may also contribute significantly to the development of in-stent restenosis. In a previous model

we showed that the level of VSMC luminal ingrowth, i.e intimal hyperplasia, is significantly higher in low compliance tissue engineered blood vessels given that reduction of cyclic strain from its physiological value increases VSMC proliferation and reduces their apoptosis rate (Zahedmanesh and Lally 2012; Colombo 2009). As such deviation of the cyclic strain from the homeostatic values due to stenting can contribute to the development of in-stent restenosis. Thicker strut stents are less compliant compared to thinner strut stents and hence could reduce the value of cyclic strain more significantly which may lead into higher proliferation of VSMCs. Also, due to the stress-stiffening response of arteries, expansion of stents to higher diameters leads to higher wall stiffening and hence reduces the value of cyclic strain within the arterial wall. As such more exhaustive 3D FE models of stent deployment including contact mechanics between full stent and artery are required to study the changes in the value of cyclic strain and to better estimate the arterial stresses. However, due to the computational limitations related to the ABM simulations in this study an axisymmetric model of a single strut is utilised. Each ABM simulation presented in this study required approximately up to 6 hours to execute on a single core 2.4 GHz processor. Extending the model to a more elaborate 3D model of full stent-artery interaction will dramatically increase the number of agents in the ABM simulations and will requires significant computational resources. *The current 2D axisymmetric model can provide valuable information regarding the localised response of arteries to stent struts, however, a 3D model would be necessary to more fully investigate a range of different stent design parameters.* Parallel processing techniques could potentially be utilised in the future to extend the models to 3D.

## 5. Conclusion

In this study a mechanistic multiscale mechanobiological model using agent based models coupled with finite element analysis was used to decipher the role of collagen turnover and endothelium in development of in-stent restenosis. The mechanobiological model allows new hypotheses on the mechanisms underlying the development of in-stent restenosis to be tested quantitatively and hence helps to generate key knowledge and insights into the mechanisms underlying the pathophysiology of in-stent restenosis. Specifically, the model corroborates the hypothesis that changes occurring within the collagen matrix following stent induced damage due to VSMC-collagen interaction play a key role in the long-term outcome of stent deployment procedures.

## Acknowledgements

Funding was provided by Research Foundation - Flanders under FWO postdoctoral fellowship scheme and a Science Foundation Ireland Research Frontiers Grant SFI (08/RFP/ENM1378).

## References


Absood A, Furutani A, Kawamura T, Graham LM. 2004. A comparison of oxidized LDL-induced collagen secretion by graft and aortic SMCs: role of PDGF. American Journal of Physiology- Heart and Cyrculation Physiology 287:H1200–H1206. doi: 10.1152/ajpheart.00228.2004

Adiguzel E, Ahmad PJ, Franco C, Bendeck MP. 2009. Collagens in the progression and complications of atherosclerosis. Vascular Medicine 14:73-89. doi: 10.1177/1358863X08094801

Aguilera CV, George SJ, Johnson JL, Newby AC. 2003. Relationship between type IV collagen degradation, metalloproteinase activity and smooth muscle cell migration and proliferation in cultured human saphenous vein. Cardiovascular Research 58:679-688. doi: 10.1016/S0008-6363(03)00256-6

Asanuma K, Magid R, Johnson C, Nerem RM, Galis Z. 2003. Uniaxial strain upregulates matrix-degrading enzymes produced by human vascular smooth muscle cells. American Journal of Physiology- Heart and Circulation Physiology 284:1778-1784. doi: 10.1152/ajpheart.00494.2002

Babapulle MN, Eisenberg MJ. 2002. Coated stents for the prevention of restenosis: Part I. Circulation 106:2859-2866. doi: 10.1161/01.CIR.0000038982.49640.70

Bendeck MP, Zempo N, Clowes AW, Galardy RE, Reidy MA. 1994. Smooth muscle cell migration and matrix metalloproteinase expression after arterial injury in the rat. Circulation Research 75: 539-545. doi: 10.1161/01.RES.75.3.539

Boyle CJ, Lennon AB, Prendergast PJ. 2011. In silico prediction of the mechanobiological response of arterial tissue: application to angioplasty and stenting. *Journal of Biomechanical Engineering* 133(8): 081001. doi:10.1115/1.4004492

Boyle CJ, Lennon AB, Early M, Kelly DJ, Lally C, Prendergast PJ. 2010. Computational simulation methodologies for mechanobiological modelling: a cell-centred approach to neointima development in stents. Philosophical Transactions of the Royal Society A-Mathematical Physical and Engineering Sciences 368:2919-2935. doi: 10.1098/rsta.2010.0071

Briguori C, Sarais C, Pagnotta P. 2002. In-stent restenosis in small coronary arteries: impact of strut thickness. Journal of American College of Cardiology 40:403–409. doi: 10.1016/S0735-1097(02)01989-7

Caiazzo A, Evans D, Falcone JL, Hegewald J, Lorenz E, Stahl B, Wang D, Bernsdorf J, Chopard B, Gunn J, Hose R, Krafczyk M, Lawford P, Smallwood R, Walker D and Hoekstra AG. 2009. Towards a complex automata multiscale model of in-stent restenosis. Computational Science – ICCS 5544:705–714. doi: 10.1007/978-3-642-01970-8_70

Chabrier BE. 1996. Growth factors and vascular wall. Int Angiol 15:100-103.

Colombo A. 2009. The role of altered cyclic strain patterns on proliferation and apoptosis of vascular smooth muscle cells - implications for in-stent restenosis, PhD thesis, Dublin City University (http://doras.dcu.ie/14917/).

De Beule M, Mortier P, Carlier SG, Verhegghe B, Van Impe R, Verdonck P. 2008. Realistic finite element-based stent design: the impact of balloon folding. J Biomech 41(2):383-389. doi: 10.1016/j.jbiomech.2007.08.014

Doronzo G, Russo I, Mattiello L, Trovati M, Anfossi G. 2005. Homocysteine rapidly increases matrix metalloproteinase-2 expression and activity in cultured human vascular smooth muscle cells. Thrombosis and Haemostasis 94(6):1285-93. doi: 10.1160/TH05–04–0221.

Duraiswamy N, Schoephoerster RT, Moreno MR, Moore JE Jr. 2007. Stented artery flow patterns and their effects on the artery wall. Annual Review of Fluid Mechanics 39: 357–382. doi: 10.1146/annurev.fluid.39.050905.110300

Early M, Lally C, Prendergast PJ, Kelly DJ. 2008. Stresses in peripheral arteries following stent placement: a finite element analysis. Computer Methods in Biomechanics and Biomedical Engineering 12:25–33. doi:10.1080/10255840802136135

Evans D, Lawford P, Gunn J, Walker D, Hose R, Smallwood R, Chopard B, Krafczyk M, Bernsdorf J, Hoekstra A. 2008. The Application of Multiscale Modelling to the Process of Development and Prevention of Stenosis in a Stented Coronary Artery. Philosophical Transactions of the Royal Society A 366:3343–3360. doi: 10.1098/rsta.2008.0081

Garasic JM, Edelman ER, Squire JC, Seifert P, Williams MS, Rogers C. 2000. Stent and artery geometry determine intimal thickening independent of arterial injury. Circulation 101:812-818. doi: 10.1161/01.CIR.101.7.812

George SJ, Zaltsman AB, Newby AC. 1997. Surgical preparative injury and neointima formation increase MMP-9 expression and MMP-2 activation in human saphenous vein. Cardiovascular Research 33: 447–459. doi: 10.1016/S0008-6363(96)00211-8

Gijsen FJH, Migliavacca F, Schievano S, Socci L, Petrini L, Thury A, Wentzel JJ, van der Steen AFW, Serruys PWS, Dubini G. 2008. Simulation of stent deployment in a realistic human coronary artery. BioMedical Engineering OnLine 6:7–23. doi: 10.1186/1475-925X-7-23

Grote K, Flach I, Luchtefeld M, Akin E, Holland SM, Drexler H, Schieffer B. 2003.. Mechanical stretch enhances mRNA expression and proenzyme release of matrix metalloproteinase-2 (MMP-2) via NAD(P)H oxidase-derived reactive oxygen species. Circulation Research 92: 80e– 86e. doi: 10.1161/ 01.RES.0000077044.60138.7C

Gunn J, Arnold N, Chan KH, Shepherd L, Cumberland DC, Crossman DC. 2002. Coronary artery stretch versus deep injury in the development of in-stent neointima. Heart 88: 401–405. doi:10.1136/heart.88.4.401

Hahn MS, Mchale MK, Wang E, Schmedlen RH, West JI. 2007. Physiologic pulsatile flow bioreactor conditioning of poly(ethyleneglycol)-based tissue engineered vascular grafts. Annals of Biomedical Engineering 35(2):190–200. doi: 10.1007/s10439-006-9099-3

Hirose M, Kosugi H, Nakazato K, Hayashi T. 1999. Restoration to a quiescent and contractile phenotype from a proliferative phenotype of myofibroblasts-like human aortic smooth muscle cells by culture on type IV collagen gels. J Biochem 125:991-1000.

Hoffmann R, Mintz GS. 2000. Coronary in-stent restenosis—predictors, treatment and prevention. European Heart Journal 21:1739–1749. doi: 10.1053/euhj.2000.2153

Holzapfel GA, Stadler M, Gasser TC. 2005a. Changes in the mechanical environment of stenotic arteries during interaction with Stents: computational assessment of parametric stent designs. Journal of Biomechanical Engineering –Transactions of ASME 127:166–180. doi: 10.1115/1.1835362

Holzapfel GA, Sommer G, Gasser CT, Regitnig P. 2005b. Determination of layer-specific mechanical properties of human coronary arteries with nonatherosclerotic intimal thickening and related constitutive modelling. American Journal of Physiology—Heart and Circulatory Physiology 289, 2048–2058. doi: 10.1152/ajpheart.00934.2004

Houbballah R, Robaldo A, Albadawi H, Titus J, LaMuraglia GM. 2011. A novel model of accelerated intimal hyperplasia in the pig iliac artery. Int J Exp Path 92:422–427. doi: 10.1111/j.1365-2613.2011.00790.x

Ilachinski A. 2001.. Cellular automata: a discrete universe. Singapore: World Scientific.

Jaffe EA, Nachman RL, Becker CG, Miinick CR. 1973. Culture of human endothelial cells derived from umbilical veins, identification by morphologic and immunologic criteria. The Journal of Clinical Investigation 52:2745-2756. doi: 10.1172/JCI107470

James TW, Wagner R, White LA, Zwolak RM, Brinkerhoff CE. 1993. Induction of collagenase gene expression by mechanical injury in avascular smooth muscle cell derived cell line. Journal of Cellular Physiology 157:426– 437. doi: 10.1002/jcp.1041570227

Kastrati A, Mehilli J, Dirschinger J, Dotzer F, Schühlen H, Neumann FJ, Fleckenstein M, Pfafferott C, Seyfarth M, Schömig A. 2001. Intracoronary stenting and angiographic results: strut thickness effect on restenosis outcome (ISAR-STEREO) trial. Circulation 103:2816– 2821. doi:10.1016/S0735-1097(03)00119-0

Kim YJ, Sah RL, Doong JY, Grodzinsky AJ. 1988. Fluorometric assay of DNA in cartilage explants using Hoechst 33258. Analytical Biochemistry 174:168-176. doi: 10.1016/0003-2697(88)90532-5

Kim YS, Galis ZS, Rachev A, Han HC, Vito RP. 2009. Matrix metalloproteinase-2 and -9 are associated with high stresses predicted using a nonlinear heterogeneous model of arteries. J Biomech Eng 131:011009.

Kleiner DE,Tuuttila A, Tryggvason K, Stetler-Stevenson WG. 1993. Stability Analysis of Latent and Active 72-kDa Type IV Collagenase: The Role of Tissue Inhibitor of Metalloproteinases-2 (TIMP-2). Biochemistry 32:1583-1592. doi: 10.1021/bi00057a024

Kornowski R, Hong MK, Tio FO, Bramwell O, Wu H, Leon MB. 1998. In-stent restenosis: contributions of inflammatory responses and arterial injury to neointimal hyperplasia. Journal of the American College of Cardiology 31(1):224-230. doi: 10.1016/S0735-1097(97)00450-6

Lally C, Dolan F, Prendergast PJ. 2005. Cardiovascular Stent Design and Vessel Stresses: A Finite Element Analysis. Journal of Biomechanics 38:1574–1581. doi:10.1016/j.jbiomech.2004.07.022

Le J, Dauchot P, Perrot JL, Cambazard F, Frey J, Chamson A. 1999. Quantitative zymography of matrix metalloproteinases by measuring hydroxyproline: application to gelatinases A and B. Electrophoresis 20:2824–2829. doi: 10.1002/(SICI)1522-2683(19991001)

Lindner V, Reidy MA. 1991. Proliferation of smooth muscle cells after vascular injury is inhibited by an antibody against basic fibroblast growth factor. Proceedings of the National Academy of Sciences of the united states of America 88(9):3739–3743.

Lowe HC, Oesterle SN, Khachigian LM. 2002. Coronary in-stent restenosis: Current status and future strategies. J Am Coll Cardiol 39:183-193. doi: 10.1016/S0735-1097(01)01742-9

Masselot A, Chopard B. 1998. A lattice Boltzmann model for particle transport and deposition. Europhys. Lett. 42: 259–262.

Matsusaki M, Amemori S, Kadowaki K, Akashi M. 2011. Quantitative 3D Analysis of Nitric Oxide Diffusion in a 3D Artery Model Using Sensor Particles. Angew Chem Int Ed 50(33):7557–7561. DOI: 10.1002/anie.201008204

Migliavacca F, Petrini L, Colombo M, Auricchio F, Pietrabissa R. 2002. Mechanical behavior of coronary stents investigated through the finite element method. Journal of Biomechanics 35: 803–811.

Migliavacca F, Petrini L, Massarotti P, Schievano S, Auricchio F, Gabriele Dubini . 2004.. Stainless and shape memory alloy coronary stents: a computational study on the interaction with the vascular wall. Biomechanics and Modeling in Mechanobiology 2:205-217. doi: 10.1007/s10237-004-0039-6

Mitra AK, Agrawal DK. 2006. In stent restenosis: bane of the stent era. Journal of Clinical Pathology 59:232–239. doi:10.1136/jcp.2005.025742

Monaco S, Sparano V, Gioia M, Spardella D, Di Pierro D, Marini S, Coletta M. 2006. Enzymatic processing of collagen IV by MMP-2 (gelatinase A) affects

neutrophil migration and it is modulated by extracatalytic domains. Protein Science: 15:2805–2815. doi: 10.1110/ps.062430706

Morton, A.C., Crossman, D. & Gunn, J. 2004. The influence of Physical Stent Parameters Upon Restenosis. Pathological Biology 52:196–205. doi:10.1016/j.patbio.2004.03.013

Mortier P, Holzapfel GA, De Beule M, Van Loo D, Taeymans Y, Segers P, Verdonck P, Verhegghe BA. 2010. novel simulation strategy for stent insertion and deployment in curved coronary bifurcations: comparison of three drug-eluting stents. Annals of Biomedical Engineering 38(1):88-99. doi: 10.1007/s10439-009-9836-5.

Newby AC. 2006. Matrix metalloproteinases regulate migration, proliferation, and death of vascular smooth muscle cells by degrading matrix and non-matrix substrates. Cardiovascular Research 69(3):614-624. doi: 10.1016/j.cardiores.2005.08.002

Nowlan NC, Prendergast PJ. 2005. Evolution of mechanoregulation of bone growth will lead to non-optimal bone phenotypes. *Journal of Theoretical Biology* 235:408-418. doi: 10.1016/j.jtbi.2005.01.021

Ogden RW. 1972. Large deformation isotropic elasticity: on the correlation of theory and experiment for incompressible rubberlike solids. Proceedings of the Royal Society of London A- Mathematical and Physical Sciences 326: 565–584. doi: 10.1098/rspa.1972.0026

Okuno T, Andoh A, Bamba S, Araki Y, Fujiyama Y, Fujiyama M, Bamba T. 2002. Interleukin-1beta and tumor necrosis factor-alpha induce chemokine and matrix metalloproteinase gene expression in human colonic subepithelial myofibroblasts. Scandinavian Journal of Gastroenterology 37:317–324.

Pache J, Kastrati A, Mehilli J, Schühlen H, Dotzer F, Hausleiter J, Fleckenstein M, Neumann FJ, Sattelberger U, Schmitt C, Müller M, Dirschinger J, Schömig A. 2003. Intracoronary Stenting and Angiographic Results: Strut Thickness Effect on Restenosis Outcome (ISAR-STEREO-2), Trial. Journal of the American College of Cardiology 41:1283–1288. doi: 10.1016/S0735-1097(03)00119-0

Palmaz JC, Sibbitt RR, Reuter SR, Tio FO, Rice WJ. 1985. Expandable intraluminal graft: a preliminary study: work in progress. Radiology 156:73-77.

Peirce SM, Van Gieson EJ, Skalak TC. 2004. Multicellular simulation predicts microvascular patterning and in silico tissue assembly. The FASEB Journal. doi: 10.1096/fj.03-0933fje

Pericevic I, Lally C, Toner D, Kelly DJ. 2009. The influence of plaque composition on underlying arterial wall stress during stent expansion: The case for lesion-specific stents. Med Eng Phys 31:428-33. doi:10.1016/j.medengphy.2008.11.005

Reidy MA, Lindner V. 1991. Basic FGF and growth of arterial cells. Annals of the New York Academy of Sciences 638:290-299. doi: 10.1111/j.1749-6632.1991.tb49039.x

Schlumberger W, Thie M, Rauterberg J, Robenek H. 1991. Collagen synthesis in cultured aortic smooth muscle cells. Modulation by collagen lattice culture, transforming growth factor- beta 1, and epidermal growth factor. Arterioscler Thromb 11:1660–1666. doi: 10.1161/01.ATV.11.6.1660

Schwartz RS, Holmes DR. 1994. Pigs, dogs, baboons, and man—lessons for stenting from animal studies. Journal of Interventional Cardiology 7: 355–368. doi: 10.1111/j.1540-8183.1994.tb00469.x

Schwartz RS, Huber KC, Murphy JG, Edwards WD, Camrud AR, Vlietstra RE, Holmes DR. 1992. Restenosis and the proportional neointimal response to coronary artery injury: Results in a porcine model. Journal of the American College of Cardiology 19: 267–274. doi: 10.1016/0735-1097(92)90476-4

Southgate KM, Fisher M, Banning AP, Thurston VJ, Baker AH, Fabunmi RP, Groves PH, Davies M, Newby AC. 1996. Upregulation of basement-membrane-degrading metalloproteinase secretion following balloon angioplasty of pig carotid arteries. Circulation Research 79:1177–11 87. doi: 10.1161/01.RES.79.6.1177

Tahir H, Hoekstra AG, Lorenz E, Lawford PV, Hose DR, Gunn J, Evans DJW. 2011. Multi-scale simulations of the dynamics of in-stent restenosis: impact of stent deployment and design. Interface Focus. doi:10.1098/rsfs.2010.0024

Terashima M, Rathore S, Suzuki Y, Nakayama Y, Kaneda H, Nasu K, Habara M, Katoh O, Suzuki T. 2009. Accuracy and Reproducibility of Stent-Strut Thickness Determined by Optical Coherence Tomography. J Invasive Cardiol 21:602–605.

Thorne BC, Hayenga HN, Humphrey JD, Peirce SM. 2011. Toward a multi-scale computational model of arterial adaptation in hypertension: verification of a

multi-cell agent-based model. Frontiers in Physiology 2:20. doi: 10.3389/fphys.2011.00020

Thyberg J, Blomgren K, Roy J, Tran PK, Hedin A. 1997. Phenotype modulation of smooth muscle cells after arterial injury is associated with changes in the distribution of laminin and fibronectin. J Histochem Cytochem 45:837-846. doi: 10.1177/002215549704500608

Timmins LH, Moreno MR, Meyer CA, Criscione JC, Rachev A, Moore JE Jr. 2007. Stented artery biomechanics and device design optimization. Medical and Biological Engineering and Computing 45(5):505–513. doi: 10.1007/s11517-007-0180-3

Timmins LH, Miller MW, Clubb FJ Jr, Moore JE Jr. 2011. Increased artery wall stress post-stenting leads to greater intimal thickening. Laboratory Investigation 91: 955–967

Tracy RE. 1997. Declining density of intimal smooth muscle cells as a precondition for atheronecrosis in the coronary artery on VSMC density. Virchows Arch 430:155-162. doi: 10.1007/BF01008037

Van Beusekom HMM, Serruys PW. 2010. Drug-Eluting Stent Endothelium: Presence or Dysfunction. J Am Coll Cardiol Intv 3:76-77. doi:10.1016/j.jcin.2009.10.016

Von der Mark K. 1981. Localization of collagen types in tissues. International Reviews of Connective Tissue Research 9:265–324.

Walker DC, Southgate J, Hill G, Holcombe M, Hose DR, Wood SM, MacNeil S, Smallwood RH. 2004. The epitheliome: agent-based modelling of the social behaviour of cells. Biosystems 76: 89–100. doi: 10.1016/j.biosystems.2004.05.025

Wang WQ, Liang DK, Yang DZ, Qi M. 2006. Analysis of the transient expansion behavior and design optimization of coronary stents by finite element method. Journal of Biomechanics 39:21–32. doi: 10.1016/j.jbiomech.2004.11.003

Welt FG, Rogers C. 2002. Inflammation and restenosis in the stent era. Arteriosclerosis, Thrombosis and Vascular Biology 22(11):1769–1776. doi: 10.1161/01.ATV.0000037100.44766.5B

Wentzel JJ, Krams R, Schuurbiers JCH, Oomen JA, Kloet J, van der Giessen WJ, Serruys PW, Slager CJ. 2001. Relationship between neointimal thickness and

shear stress after wallstent implantation in human coronary arteries. Circulation 103:1740–1745. doi: 10.1161/01.CIR.103.13.1740

Wentzel JJ, Whelan DM, van der Giessen WJ, van Beusekom HMM, Andhyiswara I, Serruys PW, Slager CJ, Krams R. 2000. Coronary stent implantation changes 3-D vessel geometry and 3-D shear stress distribution. Journal of Biomechanics 33:1287–1295. doi:10.1016/S0021-9290(00)00066-X

Wieneke H, Haude M, Knocks M, Gutersohn A, von Birgelen C, Baumgart D, Erbel R. 1999. Evaluation of Coronary Stents in the Animal Model: A Review. Materialwissenschaft und Werkstofftechnik 30:809–813. doi: 10.1002/(SICI)1521-4052(199912)

Wooldridge M. 2002. An Introduction to multiagent systems. NY: Wiley, New York.

Wu W, Wang WQ, Yang DZ, Qi M. 2007. Stent expansion in curved vessel and their interactions: a finite element analysis. Journal of Biomechanics 40:2580–2585. doi: 10.1016/j.jbiomech.2006.11.009

Xia T, Akers K, Eisen AZ, Seltzer JL. 1996. Comparison of cleavage site specificity of gelatinases A and B using collagenous peptides. Biochim Biophys Acta 1293:259–266.

Zahedmanesh H, Lally C. 2009. Determination of the influence of stent strut thickness using the finite element method: implications for vascular injury and in-stent restenosis. Medical and Biological Engineering and Computing 47:385-393. doi: 10.1007/s11517-009-0432-5

Zahedmanesh H, Kelly D, Lally C. 2010. Simulation of a balloon expandable stent in a realistic coronary artery, Determination of the optimum modelling strategy. Journal of Biomechanics 43: 2126–2132. doi:10.1016/j.jbiomech.2010.03.050

Zahedmanesh H, Lally C. 2012. A multiscale mechanobiological model using agent based models, Application to vascular tissue engineering. Biomechanics and Modeling in Mechanobiology 11: 363-377. doi:10.1007/s10237-011-0316-0

Zahedmanesh H, PA Cahill, C Lally. 2012. Vascular stent design optimisation using numerical modelling techniques. In: Naik G. R. (Ed.) Applied Biological Engineering-Principles and Practice. InTech, ISBN 979-953-307-397-1, In Press.

**Figure Captions:**

**Figure 1:** Development of in-stent restenosis following stent deployment, taken from (Zahedmanesh et al. 2012). (A) normal artery (B) de-endothelialisation and injury of the media (C) modulation of medial VSMC phenotype and their migration and proliferation towards the lumen (D) development of in-stent restenosis (E) re-endothelialisation and differentiation of VSMCs back to the quiescent phenotype. (EC) endothelial cells, (IEL), internal elastic lamina, (s VSMCs) synthetic vascular smooth muscle cell, (c VSMC) contractile and quiescent vascular smooth muscle cell, (EEL), external elastic lamina.

**Figure 2:** Overall schematic of the mechanobiological model of in-stent restenosis.

**Figure 3:** Axisymmetric representation of the model.

**Figure 4:** Damage as a function of von Mises stresses within the artery.

**Figure 5**: Evolution of (left) MMP2 (middle) Collagen and (right) vascular smooth muscle cells, when the 0.085 mm thickness strut was deployed to a diameter of 4.7 mm (expansion ratio of 1.2). The results are shown in the reference undeformed configuration.

**Figure 6:** (left) MMP-2 synthesis by VSMCs in response to damage (right) Damage initiation due to high stresses and removal of the damage by MMPs when the 0.085 mm thickness strut was deployed to a diameter of 4.7 mm (expansion ratio of 1.2). The results are shown in the reference undeformed configuration.

**Figure 7:** The axisymmetric model of stent strut interaction with the artery, the 0.085 mm thick strut deployed to a diameter of (a) 4.3 mm (expansion ratio of 1.1), (b) 4.7 mm (expansion ratio of 1.2), (c) 5.1 mm (expansion ratio of 1.3) and (d) the 0.17mm thick strut deployed to a diameter of 4.7 mm (expansion ratio of 1.2).

**Figure 8:** The influence of depth of strut penetration on VSMCs growth and development of in stent restenosis using the 0.085 mm thickness strut. The ABM domain is shown in the reference undeformed configuration.

**Figure 9:** The influence of stent strut size on VSMC growth and development of in-stent restenosis when both struts were deployed to a diameter of 4.7 mm (expansion ratio of 1.2). The ABM domain is shown in the reference undeformed configuration.

**Figure 10**: Collagen changes and development of restenosis when the 0.085 mm thick strut was deployed to a diameter of (a) 4.3 mm (expansion ratio of 1.1), (b) 4.7 mm (expansion ratio of 1.2), and (c) 5.1 mm (expansion ratio of 1.3). The results are shown in the reference undeformed configuration.

**Figure 11**: The influence of endothelialisation on VSMC number and luminal ingrowth when the 0.085 mm thickness strut was deployed to a diameter of 4.7 mm (expansion ratio of 1.2). The ABM domain is shown in the reference undeformed configuration.

**Table Titles:**

**Table 1:** Coefficients of the Ogden hyperelastic constitutive models (Zahedmanesh & Lally 2009)

**Table 2:** Parameters used in the ABM module and their sources and rationale.

**Figures:**

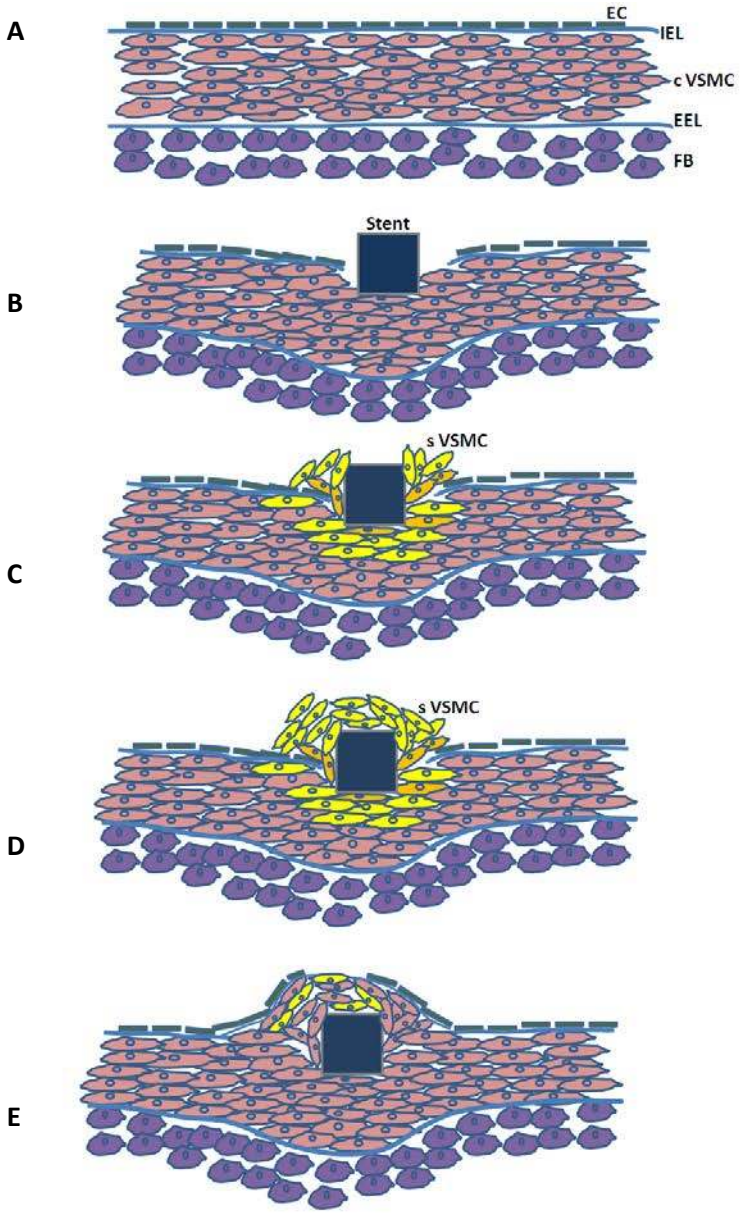


**Figure 1:** Development of in-stent restenosis following stent deployment, taken from (Zahedmanesh et al. 2012). (A) normal artery (B) de-endothelialisation and injury of the media (C) modulation of medial VSMC phenotype and their migration and proliferation towards the lumen (D) development of in-stent restenosis (E) re-endothelialisation and differentiation of VSMCs back to the quiescent phenotype. (EC) endothelial cells, (IEL), internal elastic lamina, (s VSMCs) synthetic vascular smooth muscle cell, (c VSMC) contractile and quiescent vascular smooth muscle cell, (EEL), external elastic lamina.

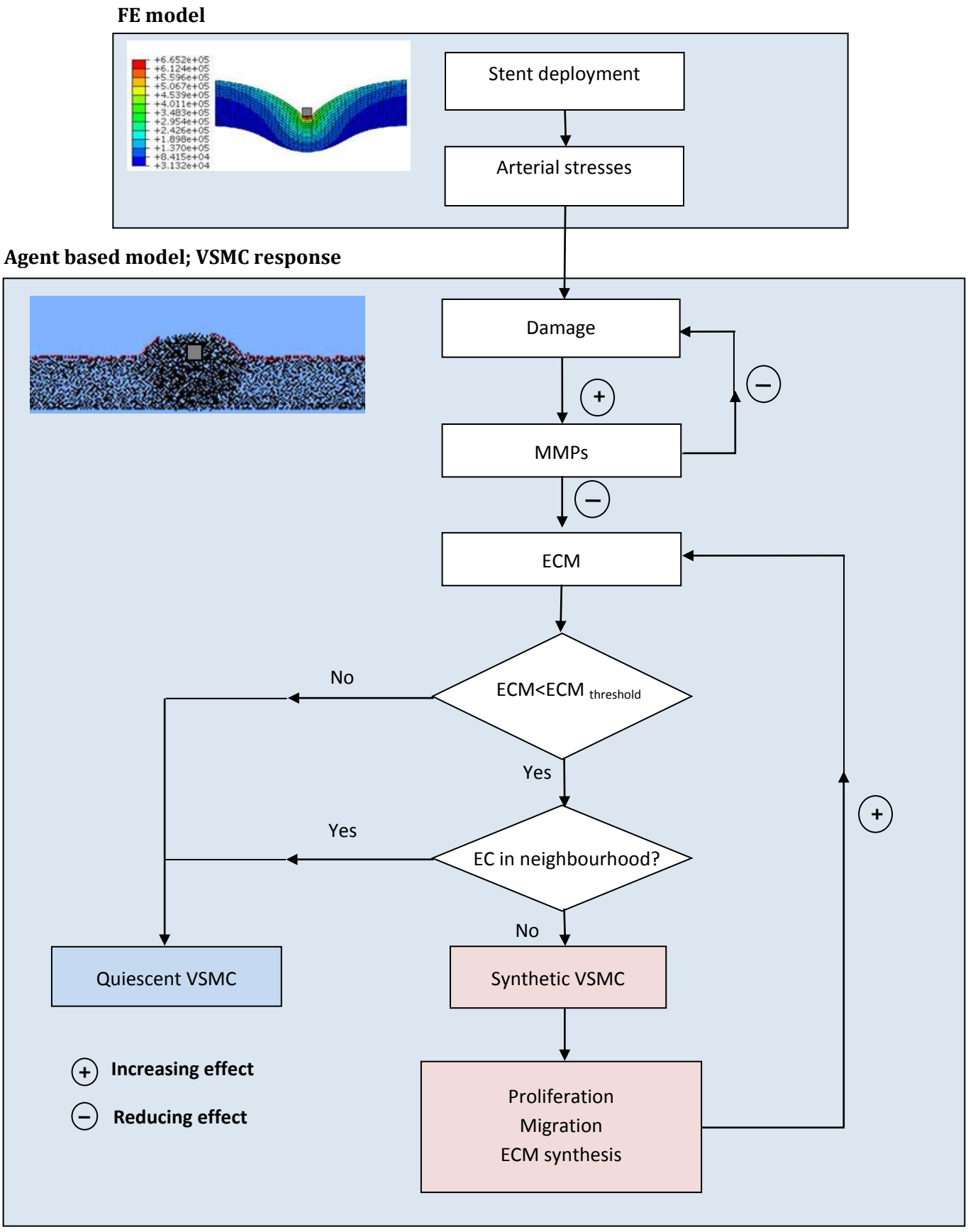


**Figure 2**: Overall schematic of the mechanobiological model of in-stent restenosis

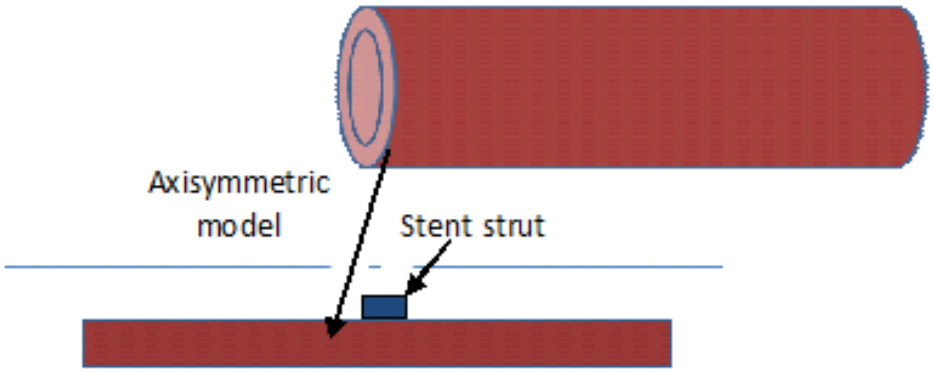


**Figure 3**: Axisymmetric representation of the model

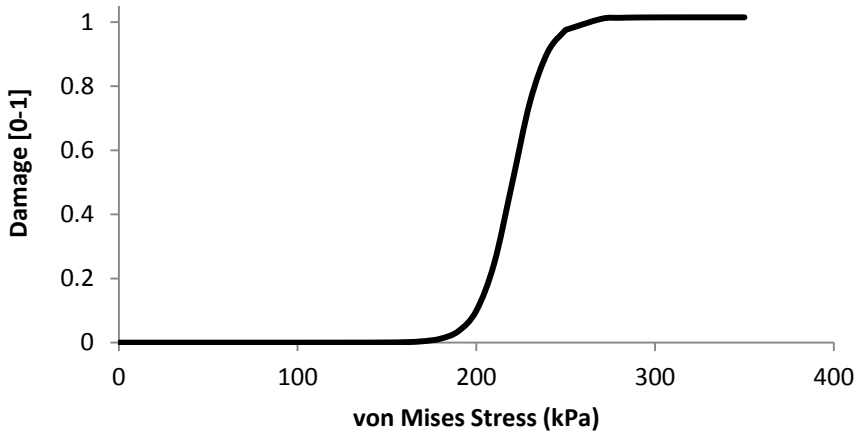


**Figure 4:** Damage as a function of von Mises stresses within the artery

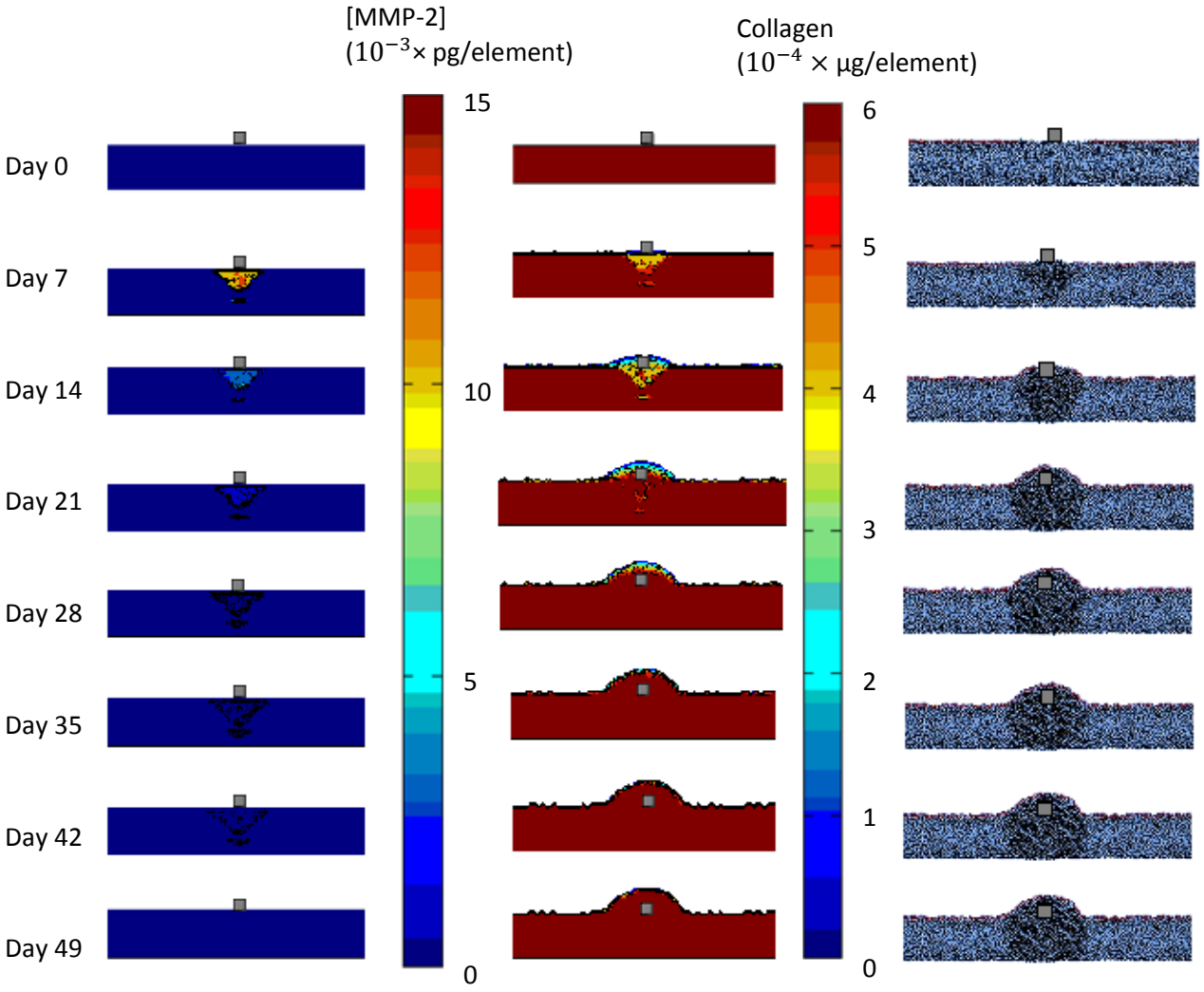


**Figure 5**: Evolution of (left) MMP2 (middle) Collagen and (right) vascular smooth muscle cells, when the 0.085 mm thickness strut was deployed to a diameter of 4.7 mm (expansion ratio of 1.2). The results are shown in the reference undeformed configuration.

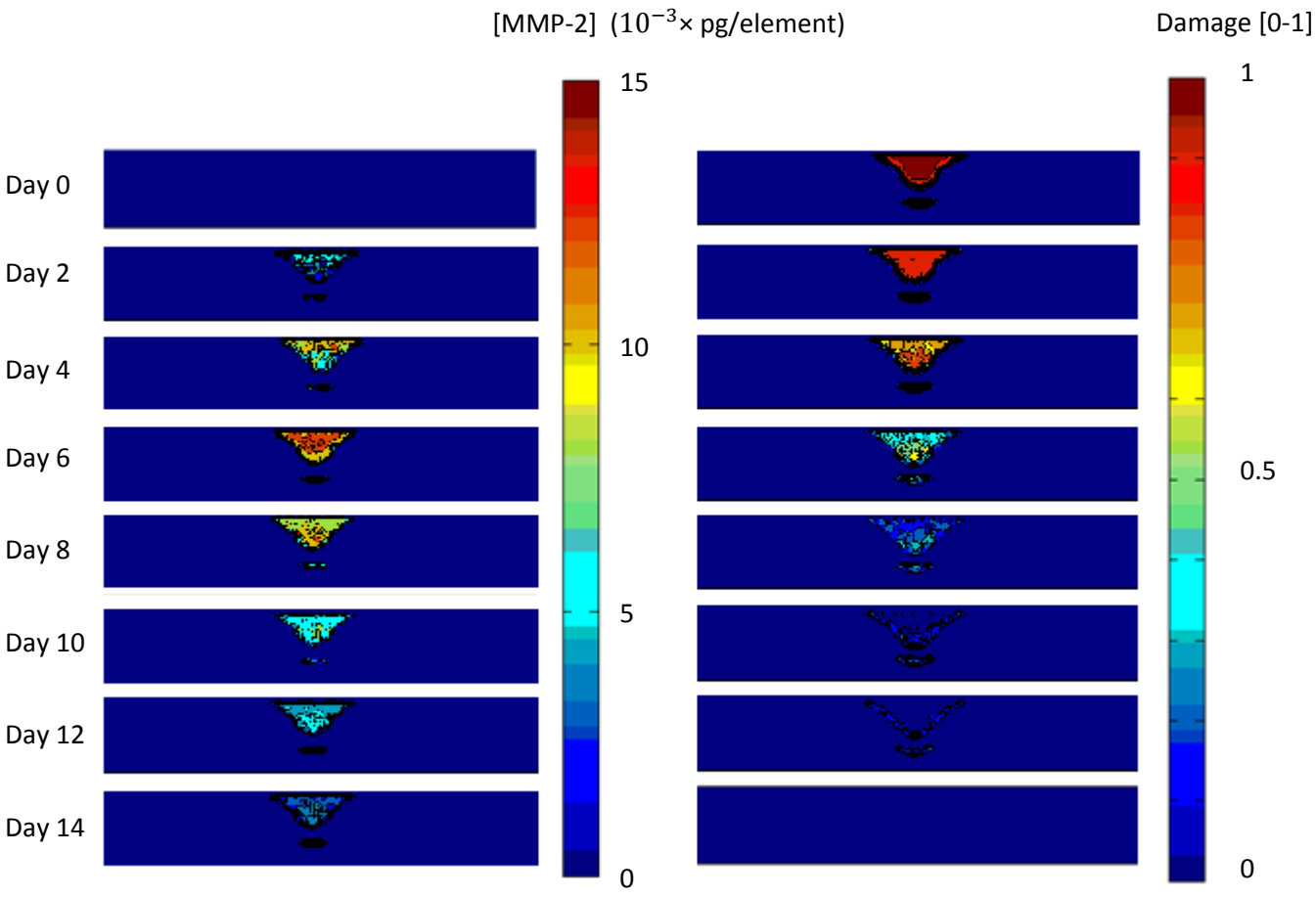


**Figure 6:** (left) MMP-2 synthesis by VSMCs in response to damage (right) Damage initiation due to high stresses and removal of the damage by MMPs when the 0.085 mm thickness strut was deployed to a diameter of 4.7 mm (expansion ratio of 1.2). The results are shown in the reference undeformed configuration.

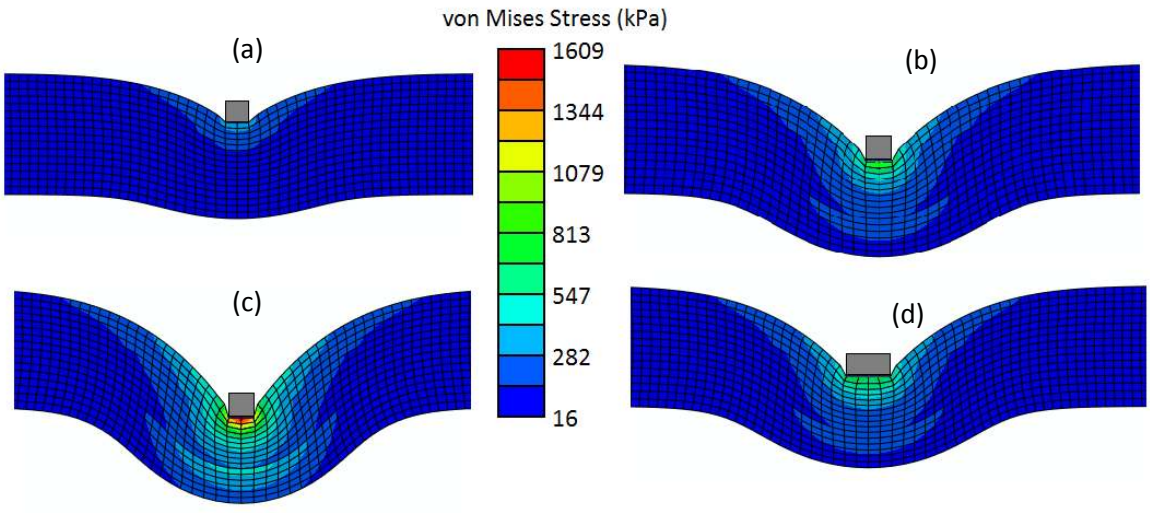


**Figure 7:** The axisymmetric model of stent strut interaction with the artery, the 0.085 mm thick strut deployed to a diameter of (a) 4.3 mm (expansion ratio of 1.1), (b) 4.7 mm (expansion ratio of 1.2), (c) 5.1 mm (expansion ratio of 1.3) and (d) the 0.17mm thick strut deployed to a diameter of 4.7 mm (expansion ratio of 1.2).

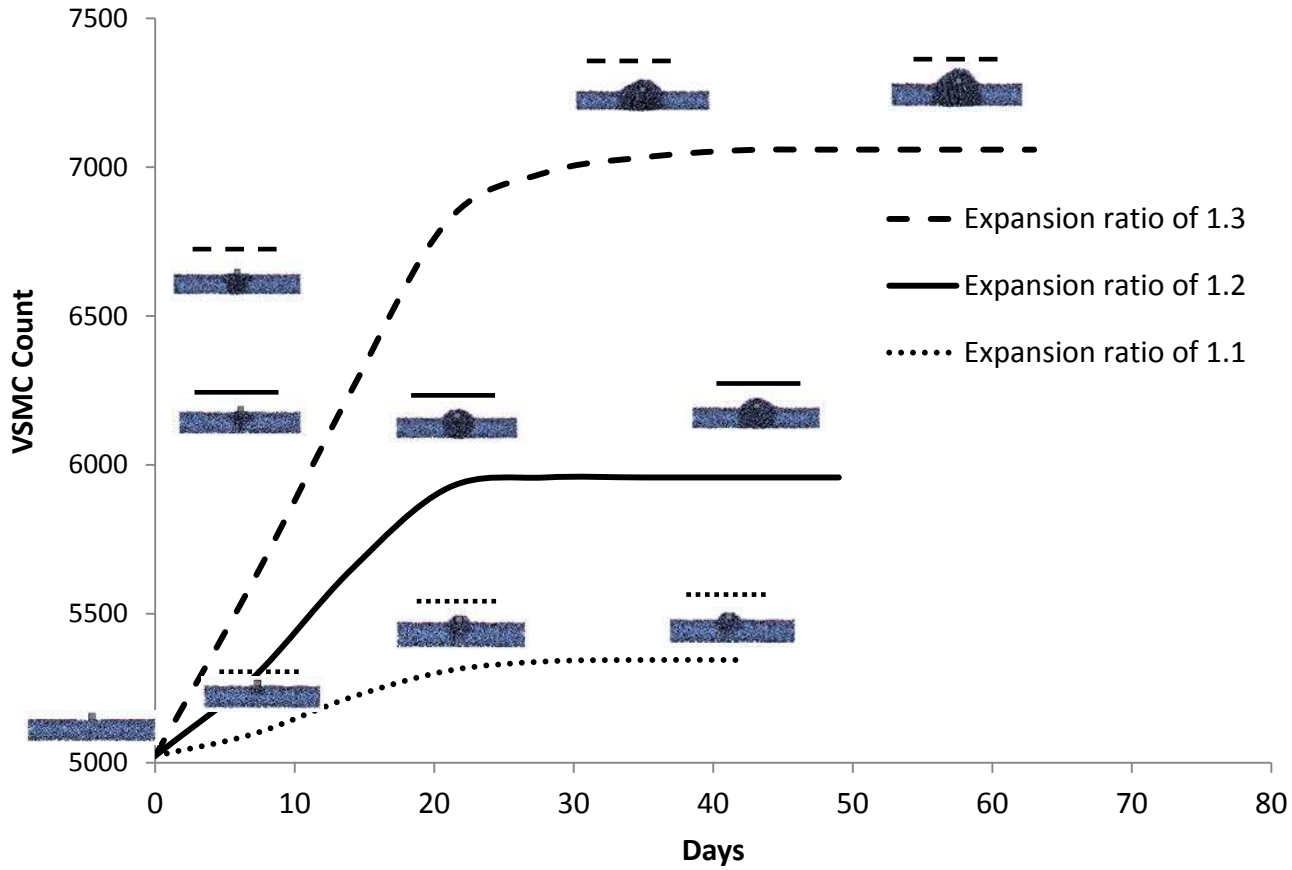


**Figure 8:** The influence of depth of strut penetration on VSMCs growth and development of in stent restenosis using the 0.085 mm thickness strut. The ABM domain is shown in the reference undeformed configuration.

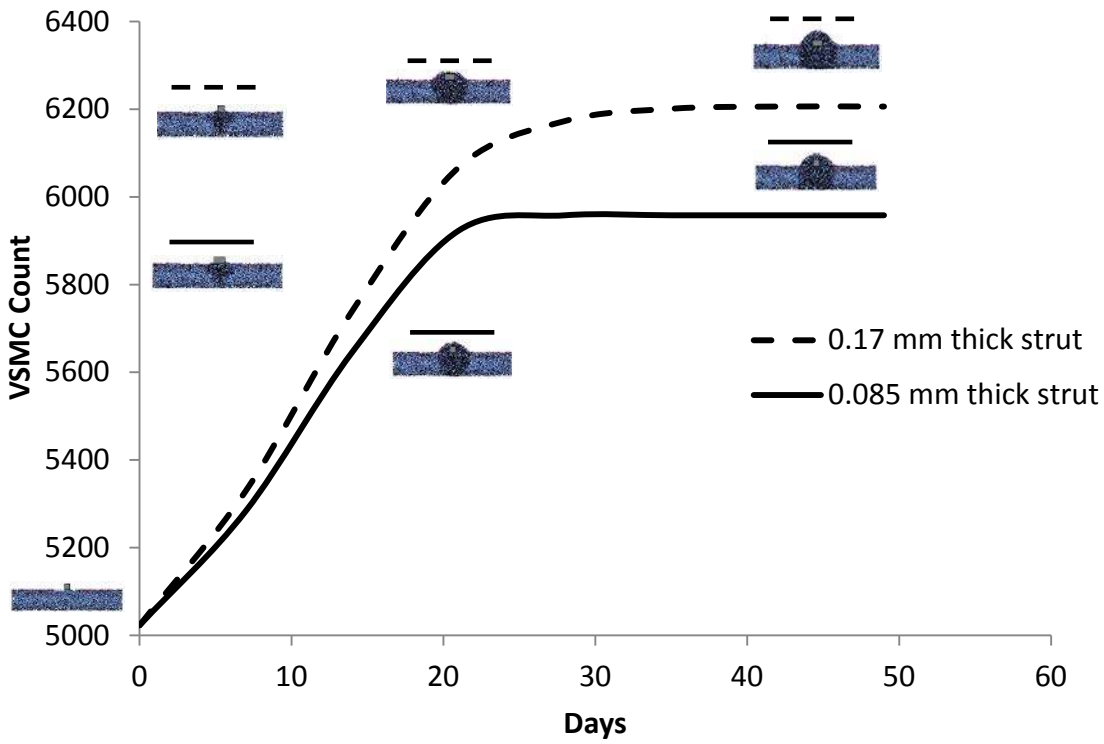


**Figure 9**: The influence of stent strut size on VSMC growth and development of in-stent restenosis when both struts were deployed to a diameter of 4.7 mm (expansion ratio of 1.2). The ABM domain is shown in the reference undeformed configuration.

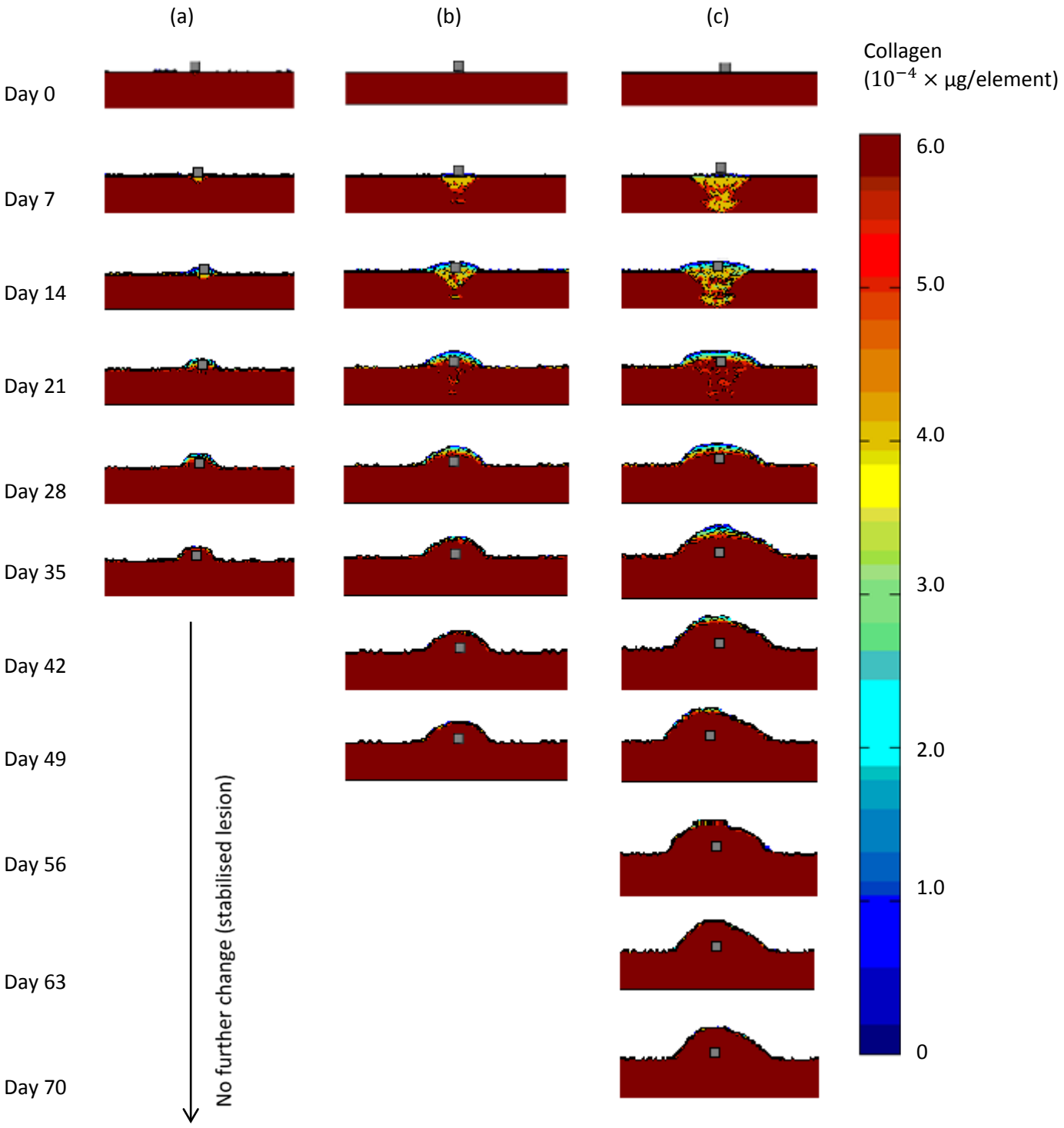


**Figure 10**: Collagen changes and development of restenosis when the 0.085 mm thick strut was deployed to a diameter of (a) 4.3 mm (expansion ratio of 1.1), (b) 4.7 mm (expansion ratio of 1.2), and (c) 5.1 mm (expansion ratio of 1.3). The results are shown in the reference undeformed configuration.

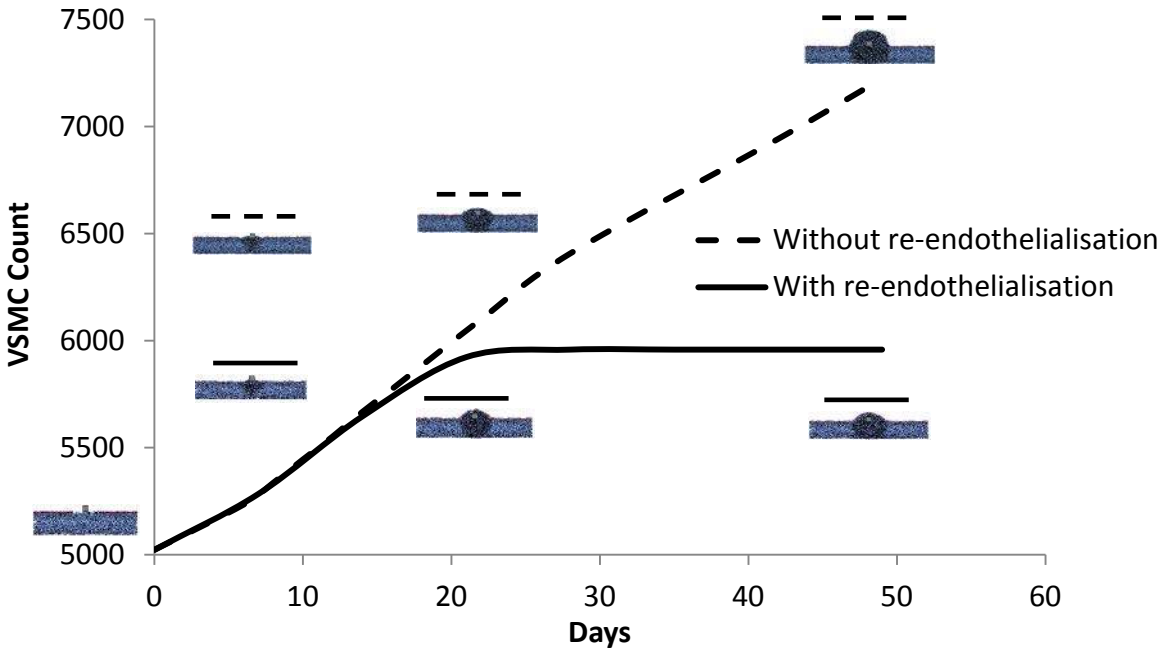


**Figure 11**: The influence of endothelialisation on VSMC number and luminal ingrowth when the 0.085 mm thickness strut was deployed to a diameter of 4.7 mm (expansion ratio of 1.2). The ABM domain is shown in the reference undeformed configuration.

| Hyperelastic constants | Media | Adventitia |
|---|---|---|
| $\mu_1$ (Pa) | -1,231,144.96 | -1,276,307.99 |
| $\mu_2$ (Pa) | 785,118.59 | 846,408.08 |
| $\mu_3$ (Pa) | 453,616.46 | 438,514.84 |
| $\alpha_1$ | 16.59 | 24.63 |
| $\alpha_2$ | 16.65 | 25.00 |
| $\alpha_3$ | 16.50 | 23.74 |

**Table 1**: Coefficients of the Ogden hyperelastic constitutive models (Zahedmanesh and Lally 2009)

| Parameter | Value | Reference |
|---|---|---|
| MMP synthesis by VSMC | $MMP2\left(\frac{(pg/cell)}{hour}\right) = \frac{0.0000916}{1 + 3462 \times e^{(-16.3 \times dmg)}}$ where dmg is damage value with a range of 0 to 1. | Kim et al., 2009; Okuno et al., 2002; Thorne et al., 2011 |
| ECM degradation rate | 410 pg collagen/pg MMP2/hour | Xia et al. 1996; Le et al., 1999; Thorne et al. 2011 |
| Damage removal by MMPs | 0.661/ pg MMP2/hour | calculated based on the fraction of ECM degraded by MMPs |
| MMP Removal | 1% MMP2/hour | Kleiner et al. 1993 |
| ECM synthesis by VSMC | 0.00899 pg collagen/hour/cell | Kim et al. 1988; Schlumberger et al., 1991; Absood et al., 2004; Thorne et al., 2011 |
| ECM threshold value for phenotype modulation | $6.2\times10^{-4}$ μg collagen/element | Hahn et al., 2007; Zahedmanesh and Lally 2012 (based on the collagen value in normal arteries) |
| Doubling time of synthetic VSMC | 43 hours | Zahedmanesh and Lally 2012 (assuming negligible cyclic strain in the damaged lesion due to low compliance of stents) |
| Maximum VSMC migration Speed: | 0.001 mm/hr | DiMilla et al., 1993; Zahedmanesh and Lally 2012 |
| Doubling time of ECs | 92 hours | Jaffe et al. 1973 |
| EC radius | 0.01787 mm | Peirce et al. 2004 |
| VSMC radius | 0.01296 mm | Peirce et al. 2004 |

**Table 2**: Parameters used in the ABM module and their sources and rationale.